IJST, Transactions of Civil Engineering, Vol. 38, No. C1+, pp 261-274
Printed in The Islamic Republic of Iran, 2014

OPTIMAL DESIGN OF CANTILEVER RETAINING WALLS USING RAY OPTIMIZATION METHOD*

A. KAVEH** AND M. KHAYATAZAD

Centre of Excellence for Fundamental Studies in Structural Engineering, School of Civil Engineering, Iran University of Science and Technology, Narmak, Tehran 16, I. R. of Iran
Email: alikaveh@iust.ac.ir

Abstract– Earth retaining structures are referred to those structures which can control backfill heights that are just about to slide. Some examples of these structures are gravity and cantilever retaining walls. The cantilever retaining walls were utilized after the introduction of the reinforced-concrete construction technique. In the previous studies, the optimization of the retaining walls has been accomplished by quasi-static methods; however, in this paper a pseudo-dynamic approach is utilized. The advantage of the pseudo-dynamic analysis is that the phase difference effects and time can be entered in the design of retaining walls as the dynamic characteristics of the earthquake loading. Here, by optimizing a cantilever retaining wall via a recently developed method, so-called Ray Optimization, the design controlling parameters are investigated. Ray Optimization method is a multi-agent optimization method which is inspired from the concept of light refraction. In this method by moving the agents to new positions, the optimal solution is found.

Keywords– Pseudo-dynamic approach, cantilever retaining wall, ray optimization

1. INTRODUCTION

Earth retaining structures are referred to those structures which can control backfill heights that are just about to slide. These structures are used when the gravity retaining walls are uneconomical. Though the retaining walls are often out of sight of the public, like other tall building structures and bridges, they have an important role in the societies.

If there is a mistake in the design of retaining walls, it causes a great deal of catastrophic damages. One can perform the analysis and design retaining walls by static, quasi-static, pseudo-dynamic and dynamic approaches. In order to design this structure by static approach, the Rankine or Coulomb theory can be utilized [1]. In this manner, the backfill thrust can be related to some coefficients, and ultimately using an equation, this pressure can be calculated. Another method that can be used is the quasi-static methods. In the quasi-static approach, the transient earthquake force and static thrust are simultaneously imposed on the retaining wall as an equivalent static force.

This method is based on the plasticity theory and is essentially an extension of the Coulomb sliding wedge theory. The pioneers of this method are Mononobe and Matsuo [2] and Okabe [3] and their work is known as Mononobe-Okabe method. In the quasi-static methods, the dynamic natural of the earthquake loading is considered to some extent. Now if one can consider some dynamic properties like phase difference effect and time in the backfill of the retaining walls, he or she will achieve a pseudo-dynamic approach. Methods like Steedman and Zeng [4] and Choudhury and Nimbalkar [5] are examples of this approach. The last method for the analysis and design of the retaining walls is dynamic one. The

*Received by the editors April 22, 2013; Accepted October 15, 2013.
**Corresponding author

performed analyses in this method are generally based on finite element method in the semi-infinite environment, thus because of high computational time, dynamic method is generally utilized for scientific purposes [6].

To obtain a design with minimum cost and time consumption, optimization methods must be used. For examples Kaveh and Behnam [7] used Charged System Search algorithm for optimization of gravity retaining walls, and Kaveh and Shakouri [8] employed harmony search algorithm for optimization of cantilever retaining walls. Both of these works use quasi-static approach for determining the active earth pressure behind the retaining walls. However, in this paper the pseudo-dynamic approach is utilized for determining this force. This optimization is performed by a new meta-heuristic method, so-called Ray optimization (RO), Ref. [9].

In this article after introducing the pseudo-dynamic approach which is offered by Choudhury and Nimbalkar [5], the concepts of this new optimization method are presented. The optimization basics of a cantilever retaining wall are gathered in section 4. In section 5, the optimal design of a cantilever retaining wall under different earthquake loading conditions is performed. The paper is concluded in section 6.

2. PSEUDO-DYNAMIC METHOD OF SEISMIC ACTIVE EARTH PRESSURE BEHIND RETAINING WALLS

A common method for determining the distribution of seismic earth pressure is Mononobe-Okabeh method [10]. This approximate method offers a linear pressure distribution behind the retaining wall and does not consider the time as a natural feature of the earthquake loading. Pseudo-dynamic approach provides a condition in which the realistic non-linear distribution of active earth pressure can be presented by considering the finite shear wave propagation. Because of the existence of the finite shear wave propagation in the problem, time and phase difference, which are two important characteristics of the earthquake loading, can have their roles in the calculation of the seismic active earth pressure. Choudhury and Nimbalkar [5] performed such analysis in which a wide range of parameters were considered. These were wall friction angle (δ), soil friction angle (φ), shear wave velocity (V_s), primary wave velocity (V_p) and horizontal and vertical ground accelerations a_h and a_v, respectively.

The following definitions and concepts are taken mainly from Ref. [5].

Consider the fixed base vertical rigid retaining wall AB of height H as shown in Fig. 1. The wall supports a cohesionless backfill material with horizontal ground. In the present study, two types of wave velocities are considered:

1. The shear wave velocity $V_s = \sqrt{G/\rho}$, with ρ and G being the density and shear modulus of the backfill material.

2. The primary wave velocity $V_p = \sqrt{\dfrac{G(2-2\upsilon)}{\rho(1-2\upsilon)}}$, with υ being the Poisson's ratio of the backfill.

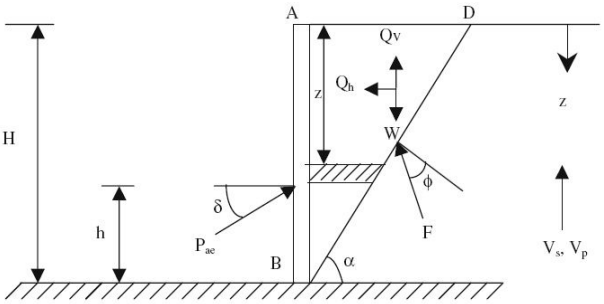

Fig. 1. Model of the retaining wall considered for computation of pseudo dynamic active earth pressure [5]

The shear waves are assumed to act within the soil media due to earthquake loading. For most geological materials $V_p / V_s = 1.87$, Ref. [11]. The period of lateral shaking is considered in the analysis as $T = \frac{2\pi}{\omega} = \frac{4H}{V_s}$, where ω is the angular frequency [10]. A planer rupture surface inclined at an angle α with the horizontal is considered in the analysis.

If the base of the wall is subjected to harmonic horizontal seismic acceleration of amplitude $a_h g$, where g is the acceleration due to gravity and harmonic vertical seismic acceleration of amplitude $a_v g$, the acceleration at any depth z and time t, below the top of the wall can be expressed as:

$$\begin{aligned} a_h[z,t] &= a_h.sin[w(t-\frac{H-z}{V_s})] \\ a_v[z,t] &= a_v.sin[w(t-\frac{H-z}{V_p})] \end{aligned} \tag{1}$$

After some calculations, Choudhury and Nimbalkar define the seismic active earth pressure coefficient K_{ae} as:

$$\begin{aligned} K_{ae} &= \frac{sin(\alpha-\phi)}{tan\alpha\, cos(\delta+\phi-\alpha)} + \frac{k_h}{2\pi^2 tan\alpha}\left(\frac{TV_s}{H}\right)\times\frac{cos(\alpha-\phi)}{cos(\delta+\phi-\alpha)}\times m_1 \\ &- \frac{k_v}{2\pi^2 tan\alpha}\left(\frac{TV_p}{H}\right)\times\frac{sin(\alpha-\phi)}{cos(\delta+\phi-\alpha)}\times m_2 \\ m_1 &= \left[2\pi cos 2\pi\left(\frac{t}{T}-\frac{H}{TV_s}\right)+\left(\frac{TV_s}{H}\right)\left(sin 2\pi\left(\frac{t}{T}-\frac{H}{TV_s}\right)-sin 2\pi\left(\frac{t}{T}\right)\right)\right] \\ m_2 &= \left[2\pi cos 2\pi\left(\frac{t}{T}-\frac{H}{TV_p}\right)+\left(\frac{TV_p}{H}\right)\left(sin 2\pi\left(\frac{t}{T}-\frac{H}{TV_p}\right)-sin 2\pi\left(\frac{t}{T}\right)\right)\right] \end{aligned} \tag{2}$$

where k_h and k_v are a_h/g and a_v/g , respectively. Finally the seismic active earth pressure P_{ae} can be calculated by:

$$P_{ae} = \frac{1}{2}K_{ae}\gamma H^2 \tag{3}$$

where γ is the unit weight of the backfill. For obtaining the maximum value of K_{ae}, it is necessary to maximize Eq. (2) with respect to t/T and α (see Appendix A).

By differentiating Eq. (3), the seismic active earth pressure distribution is obtained as:

$$\begin{aligned} p_{AE}(t) &= \frac{\gamma z}{tan(\alpha)}\frac{sin(\alpha-\phi)}{cos(\delta+\phi-\alpha)} + \frac{k_h\gamma z}{tan(\alpha)}\frac{cos(\alpha-\phi)}{cos(\delta+\phi-\alpha)}sin[\omega(t-\frac{z}{V_s})] \\ &- \frac{k_v\gamma z}{tan(\alpha)}\frac{cos(\alpha-\phi)}{cos(\delta+\phi-\alpha)}sin[\omega(t-\frac{z}{V_p})] \end{aligned} \tag{4}$$

3. RAY OPTIMIZATION

Consider a light ray which is crossing the transparent medium K with the vector $\boldsymbol{V}_i^k$, Fig. 2. When this ray reaches to the point $\boldsymbol{X}_i^k$, after refracting it enters to the darker medium $K+1$ and continues its path with the vector $\boldsymbol{V}_i^{k+1}$. The direction of $\boldsymbol{V}_i^{k+1}$ is dependent on the direction of $\boldsymbol{n}$ and the refraction index ratio (n_d / n_t). For determining the direction of this vector, refer to Appendix B.

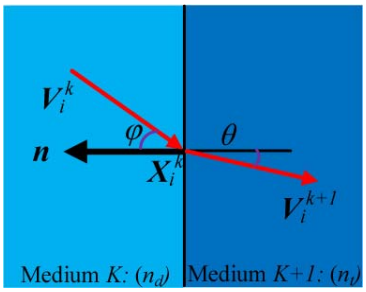

Fig. 2. Incident and refracted rays and their specifications

Ray Optimization method is a multi-agent optimization method which is inspired from the concept of light refraction [9]. In this method by moving the agents to new positions, the optimal solution is found. Thus, if the movement vector for the *i*th agent in the *k*th iteration is $\boldsymbol{V}_i^k$ and the current position of this agent is $\boldsymbol{X}_i^k$, it can be moved to its new position by $\boldsymbol{V}_i^{k+1}$. The refraction index ratio for this method is selected as 0.45. The direction of $\boldsymbol{n}$ passes through two points. The beginning point is $\boldsymbol{O}_i^k$ and final point is $\boldsymbol{X}_i^k$. $\boldsymbol{O}_i^k$ is defined as:

$$\boldsymbol{O}_i^K = \frac{(ite+k).\boldsymbol{GB}+(ite-k).\boldsymbol{LB_i}}{2.ite}, \tag{5}$$

where $\boldsymbol{GB}$ and $\boldsymbol{LB}_i$ are the so-far best position and goal function value obtained by all of the agents and *i*th agent, respectively.

If the number of variables is greater than 3, for using the ray tracing concept the search space can be divided to a number of 2D and or 3D spaces. In general, if N is an even number, the search space is divided to $(N/2)$ 2D spaces and if N is an odd number, the search space is divided to $(N-3)/2$ 2D space(s) and a one 3D space. Each of these 2D or 3D spaces is named sub-space. With this description, $\boldsymbol{V}_{i,l}^k$ is the movement vector of the *l*th sub-space which belongs to the *i*th agent in the *k*th iteration and $v_{i,j,l}^k$ is the *j*th component of the movement vector of the *l*th sub-space which belongs to *i*th agent in the *k*th iteration.

The steps of Ray Optimization algorithm are as follows:

a) Scattering and evaluation step

Based on Eq. (6), scatter the agents in the search space, randomly.

$$x_{\boldsymbol{i,j}}^{\boldsymbol{0}} = x_{j,min} + rand \times (x_{j,max} - x_{j,min}), \tag{6}$$

where, $x_{i,j}^0$ is the *j*th component of the *i*th agent. $x_{j,min}$ and $x_{j,max}$ are the allowable minimum and maximum values of the *j*th component. Here, *rand* is a random number distributed 0 through 1. After scattering, evaluate the value of goal function for each agent. Then, save the position and goal function value of each agent and the best position and goal function value of the best agent as $\boldsymbol{LB}_i$ and $\boldsymbol{GB}$, respectively.

Make a movement vector for each agent based on Eq. (7).

$$v_{\boldsymbol{i,j}}^{\boldsymbol{0}} = -1 + 2 \times rand, \tag{7}$$

where, $v_{i,j}^0$ is the *j*th component of the *i*th agent. Finally, based on the sub-space grouping, convert 2D and 3D movement vector to normalized ones.

b) Movement vector and motion refinement step

Move the agents to their new positions based on their movement vectors. If an agent violates the allowable boundaries, modify the length of its movement vector. The new length of movement vector is

equal to 0.9 times the distance of current agent position and the intersection with boundary. After modifying the movement vector, evaluate the goal function of each agent and update $\boldsymbol{GB}$ and $\boldsymbol{LB}_i$.

c) Cockshy point making and convergent step

Determine $\boldsymbol{O}_i^k$ for each agent. Then, based on Eq. (8), obtain the new movement vector. In this equation *stoch* and *d* are 0.35 and 7.5, respectively.

$$\boldsymbol{X}_{i,l}^k \neq \boldsymbol{O}_{i,l}^k \rightarrow \begin{cases} \text{w.p.}\,(1-stoch) \rightarrow \boldsymbol{V}_{i,l}^{k+1} = \boldsymbol{V}_{i,l}^{(k+1)'} \times norm(\boldsymbol{X}_{i,l}^k - \boldsymbol{O}_{i,l}^k) \\ \qquad\qquad \boldsymbol{V}_{i,l}^{(k+1)'} \text{ is determined by ray tracing.} \\ \text{w.p.}\,stoch \qquad \rightarrow \boldsymbol{V}_{i,l}^{k+1} = \dfrac{\boldsymbol{V}_{i,l}^{(k+1)'}}{norm(\boldsymbol{V}_{i,l}^{(k+1)'})} \times \dfrac{a}{d} \times rand \\ \qquad\qquad \text{Each component of } \boldsymbol{V}_{i,l}^{(k+1)'} \text{ is} \\ \qquad\qquad \text{calculated as below :} \\ \qquad\qquad v_{i,j,l}^{(k+1)'} = -1 + 2 \times rand \\ \qquad\qquad a = \sqrt{\sum_{j=1}^{n} (x_{j,max} - x_{j,min})^2} \\ \qquad\qquad n = \begin{cases} 2 & \text{for two variable groups} \\ 3 & \text{for three variable groups} \end{cases} \end{cases}$$

$$\boldsymbol{X}_{i,l}^k = \boldsymbol{O}_{i,l}^k \rightarrow \qquad \boldsymbol{V}_{i,l}^{k+1} = \frac{\boldsymbol{V}_{i,l}^k}{norm(\boldsymbol{V}_{i,l}^k)} \times rand \times 0.001 \tag{8}$$

d) Finish or redoing step

If the finishing criterion of algorithm is fulfilled the search procedure terminates, otherwise the algorithm returns to the second step and continues the search. The finishing criterion can be a specific number of iterations for obtaining the optimal solution.

4. THE BASICS OF THE OPTIMIZATION OF CANTILEVER RETAINING WALL.

In the prior sections, pseudo-dynamic analysis of Choudhury and Nimbalkar and Ray Optimization method were introduced. In this section, the basics of the optimal design of cantilever retaining wall are introduced.

In this problem, similar to Ref. [8], the cost of consumed concrete and steel is considered as goal function.

$$Q = V_{conc} \times (C_1 + C_2) + W_{steel} \times (C_3 + C_4) \tag{9}$$

By considering $\overline{Q} = Q / (C_1 + C_2)$, the goal function is converted to:

$$\overline{Q} = V_{conc} + W_{steel} \times \left(\frac{C_3 + C_4}{C_1 + C_2}\right) \tag{10}$$

Where V_{conc} and W_{steel} are the volume of concrete and the weight of reinforcement steel in the unit length (m^3/m and kg/m), C_1 and C_2 are the cost of the concrete and steel (\$/m^3 and \$/kg), C_3 and C_4 are the cost of concreting and erecting reinforcement (\$/m^3 and \$/kg). Experiences show the value of $\frac{C_1 + C_2}{C_3 + C_4}$ is in the range of 0.035 to 0.045 and in this paper 0.04 is selected. The design variables in this problem are the

thickness of top stem (T_1), the thickness of the key and bottom stem (T_2), the toe width (T_3), the heel width (T_4), the height of top stem (T_5), the footing thickness (T_6) and the key depth (T_7), Fig. 3.

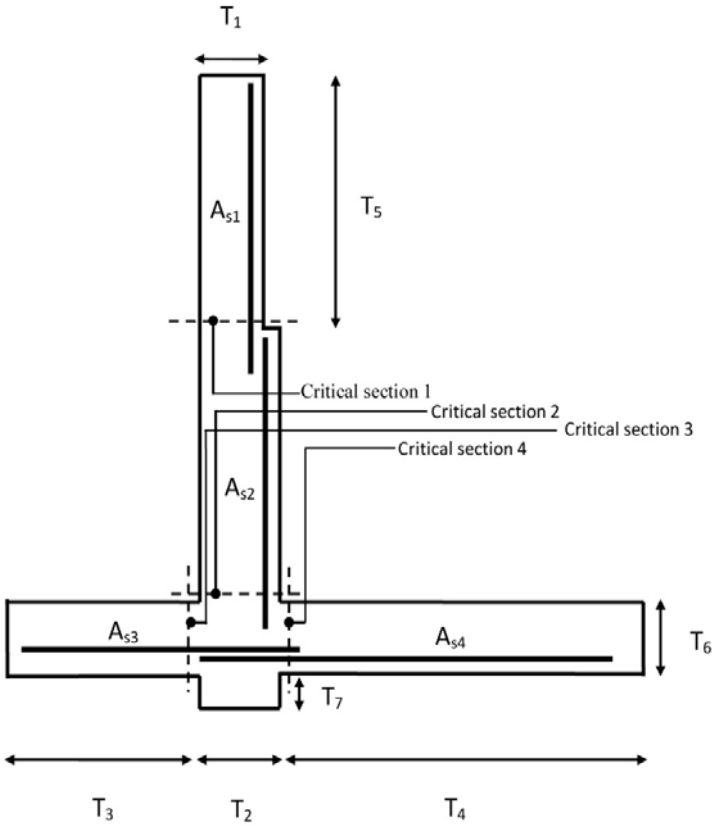

Fig. 3. Design variables and the critical sections of the cantilever retaining wall

In this problem, there are two groups of constraints. The first group is about the stability of the cantilever retaining wall under exerted forces. This group is gathered from Ref. [12]. The second one is about the shear and flexural strength which is gathered from Ref. [13]. For more details of constraints see Appendix C.

For the sake of simplicity, the penalty approach is used for constraint handling. In using the penalty function, if the constraints are not violated, the penalty will be zero; otherwise the value of the penalty is calculated by dividing the violation of the allowable limit to the limit itself.

In the process of the optimization, the required rebar based on the ultimate moment, M_u, in each critical section is calculated and then the total weight of rebar for the cantilever retaining wall is obtained.

5. A NUMERICAL EXAMPLE

In this section, the optimum design of a cantilever retaining wall under 7 earthquake dynamic loading conditions are provided. K_{ae} and the related parameters are taken from Appendix A. Based on the suggestion of Ref. [5]; $\frac{H}{TV_s}$ and $\frac{H}{TV_p}$ are selected as 0.25 and 0.1337, respectively. The allowable ranges of the design variables are given in Table 1. It should be noticed that for obtaining an optimum design in the case of $k_h=0.2$ and $k_v=0.2$, the maximum allowable value of the second variable is increased from *0.6* to *1.1m*. The stem length of the cantilever retaining wall is constant and is equal to *6.1m*. The other properties of this problem are gathered in Table 2.

Table 1. Upper and lower bounds for design variables

Design variable	T_1	T_2	T_3	T_4	T_5	T_6	T_7
Upper bound	0.3m	0.3m	0.45m	1.8m	1.5m	0.3m	0.2m
Lower bound	0.6m	0.6m	1.2m	3m	6.1m	0.9m	0.9m

Table 2. Properties of the numerical example

γ_b: Soil specific weight	20 kN/m^3
φ: Soil friction angle	30 (°)
q_u: Allowable soil pressure	300 kN/m^2
f_c': Concrete strength	25 MPa
γ_c: Concrete specific weight	24 kN/m^3
f_y: Yield stress of ribbed bar	420 MPa
γ_s: Specific weight of ribbed bar	78 kN/m^3
δ : Wall friction angle	15 (°)
Number of agents	24
Number of iterations	400

After optimization process, the results of Table 3 are obtained. $k_h=0$ and $k_v=0$ are related to the design of the cantilever retaining wall under the static loading condition. The results of Table 3 are graphically shown in Fig. 4. Based on this figure, by increasing k_h a more vigorous cantilever retaining wall is needed. But by increasing k_v, the inverse of this state becomes apparent. This behavior is predictable by considering Eq. (4). Thus in the design of the cantilever retaining walls in the prevalent conditions, ignoring the k_v is acceptable.

Table 3. The results obtained for optimum design of the cantilever retaining wall

Variable	Optimal dimensions for best result based on RO (m)						
	k_h=0.0	k_h=0.1			k_h=0.2		
	k_v=0.0	k_v=0.0	k_v=0.05	k_v=0.1	k_v=0.0	k_v=0.1	k_v=0.2
T_1	0.413	0.515	0.523	0.498	0.600	0.575	0.412
T_2	0.600	0.600	0.600	0.600	0.600	0.600	0.879
T_3	0.663	0.686	0.707	0.687	0.755	0.733	0.946
T_4	2.053	2.415	2.301	2.284	2.707	2.644	2.182
T_5	3.674	4.170	4.255	4.132	4.443	4.350	3.367
T_6	0.300	0.300	0.300	0.300	0.305	0.300	0.518
T_7	0.201	0.200	0.200	0.200	0.200	0.201	0.719
Best result	27.621	31.404	30.908	30.050	36.123	34.958	32.216

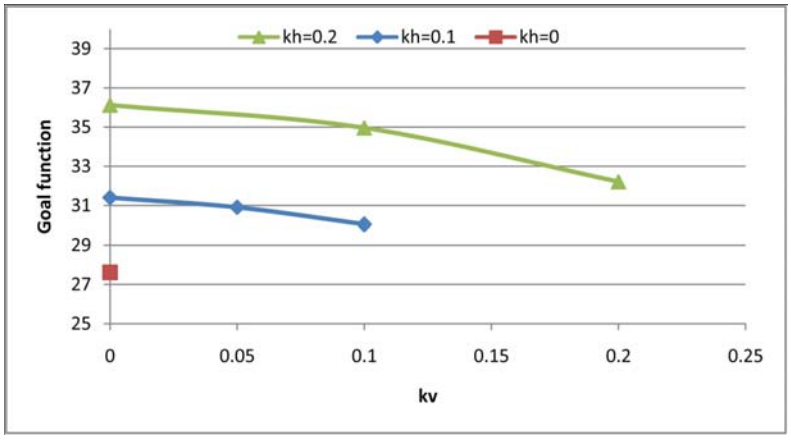

Fig. 4. Effect of k_h *and* k_v on the goal function

Figure 5 shows the convergence curve for obtaining the optimum solution. The utilized meta-heuristic methods are RO, CSS [14] and PSO.

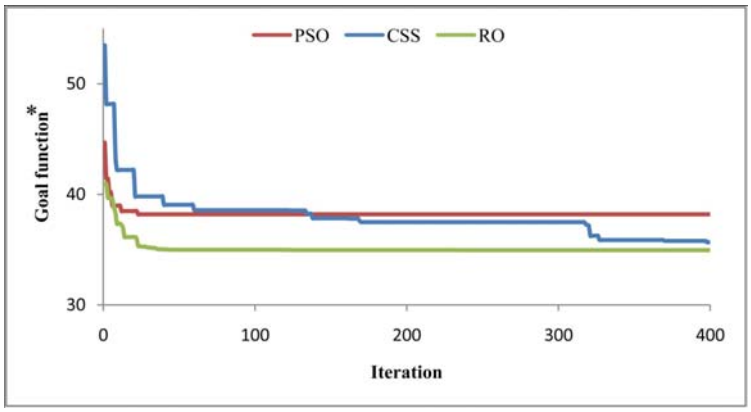

Fig. 5. Comparison of the convergence curves for the three algorithms used for the cantilever retaining wall, $k_h=0.2$ and $k_v=0.1$

Now consider the following two definitions:

$$Stability\ capacity\ ratio = \frac{Allowable\ safty\ factor}{Existing\ safty\ factor} \tag{11}$$

$$Shear\ capacity\ ratio = \frac{Existing\ shear\ force}{Allowable\ shear\ force} \tag{12}$$

By these definitions, the optimum design of the cantilever retaining wall can be investigated in more detail. Table 4 provides these details and Fig. 6 is a graphical example of this point of view.

Table 4. Capacity assessment with CR meaning the capacity ratio

Case	$k_h=0.0,k_v=0.0$	$k_h=0.1,k_v=0.0$	$k_h=0.1,k_v=0.05$	$k_h=0.1,k_v=0.1$	$k_h=0.2,k_v=0.0$	$k_h=0.2,k_v=1.0$	$k_h=0.2,k_v=0.2$
Shear CR 1	23.47%	26.59%	26.49%	25.80%	29.41%	26.28%	25.40%
Shear CR 2	41.37%	49.86%	48.13%	46.15%	60.39%	57.27%	31.51%
Shear CR 3	86.04%	90.54%	94.22%	90.51%	100.13%	99.38%	48.66%
Shear CR 4	00.00%	00.00%	00.00%	00.00%	00.00%	00.00%	40.19%
Bearing CR	99.97%	99.98%	99.94%	99.86%	100.01%	100.00%	100.02%
Sliding CR	80.42%	86.65%	90.74%	92.49%	95.68%	99.06%	100.01%
Overturning CR	56.30%	54.03%	55.58%	55.00%	54.08%	53.80%	54.58%

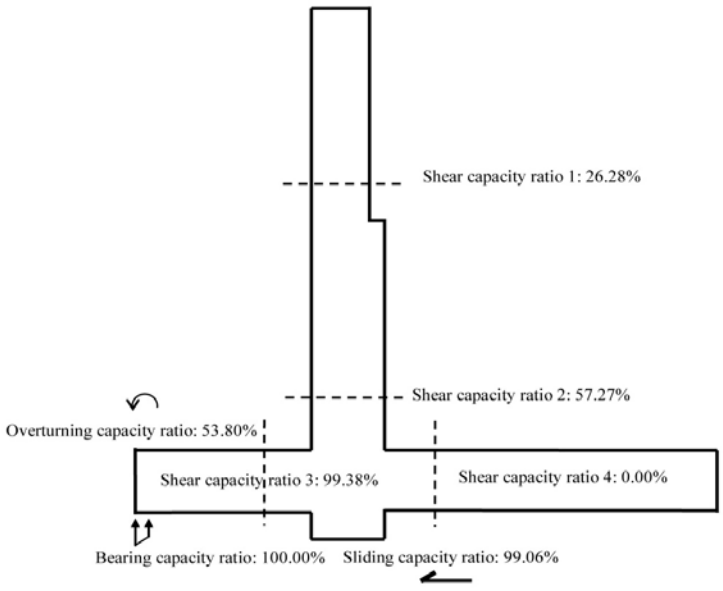

Fig. 6. Capacity assessment, $k_h=0.2$ and $k_v=0.1$

In a few cells of this table, the written capacity ratio is greater than 100%. As an example, the greatest numeral is 100.13%. However, this error is negligible, because the corresponding error of this numeral is 0.0013.

The most important controlling factor in the optimum design of cantilever retaining wall is the bearing capacity of the soil which is at the toe region. In all the cases, with a good approximation, the bearing capacity ratio is 100%. The shear capacity ratio at the toe region is the second controlling factor with average of 93% in all the cases except $k_h=0.2$ and $k_v=0.1$. Finally, the sliding capacity ratio is the last controlling factor which is increased from 80.42% to 100.01%. An important point in Table 4 is that, the shear capacity ratio at the heel region in all the cases except 7th case is 0.00%. This means the stress triangle has not entered into the heel region.

6. CONCLUDING REMARKS

The aim of the cantilever retaining wall optimization is to provide a design which not only satisfies the strength and stability constraints, but is also economical. In this paper, design of the cantilever retaining walls under various earthquake loading conditions is provided. These designs are performed by a new meta-heuristic optimization method called Ray Optimization. These designs reveal the following two results: Firstly, the bearing capacity of soil under toe region, sliding stability of cantilever retaining wall and the shear strength of the critical section in the toe region are the most important parameters in choosing the optimum design. Secondly unlike the expectation, the increase of the vertical component of the earthquake has a reverse effect on the design of the retaining walls.

Acknowledgement: The first author is grateful to the Iran National Science Foundation for the support.

REFERENCES

1. Das, B.M. (2008). *Advanced soil mechanics*. 3rd edition, New York: Taylor & Francis.
2. Mononobe, N. & Matsuo, H. (1929). On the determination of earth pressure during earthquakes. *Proc World Engineering Congress*, Tokyo, Vol. IX, pp. 85-177.
3. Okabe, S. (1926). General theory of earth pressure. *Japan Society of Civil Engineering*, Vol. 10, No. 5, pp. 1277–1323.
4. Steedman, RS. & Zeng, X. (1990). The influence of phase on the calculation of pseudo-static earth pressure on a retaining wall. *Journal of Geotechnical and Geo-environmental Engineering*, Vol. 40, No. 1, pp. 103–112.
5. Choudhury, D. & Nimbalkar, S. (2006). Pseudo Dynamic approach of seismic active earth pressure behind retaining wall. *Journal of Geotechnical and Geology Engineering*. Vol. 24, pp. 1103-1113.
6. Tanga, Y. & Chau Shioung, Y. (2001). A note on the seismic response of rigid cantilever retaining walls. *Journal of Nuclear Engineering Design*. Vol. 241, pp. 693–699.
7. Kaveh, A. & Behnam, A. F. (2013). Charged system search algorithm for the optimum cost design of reinforced concrete cantilever retaining walls. *Arabian Journal of Science and Engineering*. Vol. 38, pp. 563–570.
8. Kaveh, A. & Shakouri Mahmud Abadi, A. (2011). Harmony search based algorithms for the optimum cost design of reinforced concrete cantilever retaining walls. *International Journal of Civil Engineering*, Vol. 9, No. 1, pp. 1-8.
9. Kaveh, A. & Khayatazad, M. (2012). A new meta-heuristic: ray optimization. *Computers & Structures*. Vols. 112-113, pp. 283–294.
10. Kramer, S.L. (1996). *Geotechnical earthquake engineering*. New Jersey: Prentice Hall.
11. Das, B.M. (1993). *Principles of soil dynamics*. Massachusetts: PWS-KENT.
12. Das, B.M. (2004). *Principles of foundation engineering*. 5th ed. CL-Engineering.

13. ACI Committee 318, (2005). *Building code requirements for structural concrete (ACI 318-05) and commentary (318R-05)*. American Concrete Institute, Farmington Hills, Mich., p. 430.
14. Kaveh, A. & Talatahari, S. (2010). A novel heuristic optimization method: Charged system search, *Acta Mechanica*., Vol. 213, Nos. (3–4), pp. 267-289.
15. Mirghasemi, A. A. & Maleki Javan, M. R. (2006). Discrete element method analysis of retaining wall earth pressure in static and pseudo-static conditions. *Iranian Journal of Science and Technology, Transactions of Civil Engineering*. Vol. 30, No. B1, pp. 145-150.
16. Totonchi, A., Askari, F. & Farzaneh, O. (2012). Analytical solution of seismic active lateral force in retaining walls using stress fields. *Iranian Journal of Science and Technology, Transactions of Civil Engineering*. Vol. 36, No. 2, pp. 195-207.
17. Kaveh, A., Kalateh-Ahani, M. & Fahimi-Farzam, M. (2013). Constructability optimal design of reinforced concrete retaining walls using a multi-objective genetic algorithm. *Structural Engineering and Mechanics*, Vol. 47, No. 2, pp. 227-245.

APPENDIX A

Ray optimization method is used for maximization of K_{ae} with respect to α and t/T or t_c.

A.1. Magnitudes of K_{ae}, t_c and α for $k_v=0$

		$k_h=0.0$			$k_h=0.1$			$k_h=0.2$		
Φ (°)	δ (°)	t_c (t)	α (°)	K_{ae}	t_c (t)	α (°)	K_{ae}	t_c (t)	α (°)	K_{ae}
20	−10	0.8366	61.5561	0.5779	0.4158	57.9211	0.6619	0.4158	52.9751	0.7531
	0	0.3847	55.0000	0.4903	0.4158	50.1609	0.5747	0.4158	43.4909	0.6722
	10	0.0471	51.0568	0.4467	0.4158	45.5149	0.5340	0.4158	37.9912	0.6401
	20	0.4168	48.1495	0.4269	0.4158	42.1082	0.5198	0.4158	34.0785	0.6383
30	−15	0.3692	65.1039	0.4161	0.4201	62.3252	0.4855	0.4201	59.1001	0.5600
	0	0.1204	60.0000	0.3333	0.4201	56.3105	0.3987	0.4201	51.9607	0.4721
	15	0.0726	56.8598	0.3014	0.4201	52.5497	0.3680	0.4201	47.4551	0.4461
	30	0.9456	54.3429	0.2972	0.4201	49.4919	0.3706	0.4201	43.7647	0.4606
40	−20	0.2085	68.7680	0.2837	0.4246	66.4034	0.3386	0.4246	63.8424	0.3975
	0	0.7630	65.0000	0.2174	0.4246	61.9018	0.2663	0.4246	58.4855	0.3211
	20	0.5737	62.6013	0.1994	0.4246	58.9527	0.2496	0.4246	54.8821	0.3081
	40	0.7351	60.4258	0.2102	0.4246	56.1987	0.2698	0.4246	51.4217	0.3430

A.2. Magnitudes of K_{ae}, t_c and α for $k_v=0.5\ k_h$

		$k_h=0.0$			$k_h=0.1$			$k_h=0.2$		
Φ (°)	δ (°)	t_c (t)	α (°)	K_{ae}	t_c (t)	α (°)	K_{ae}	t_c (t)	α (°)	K_{ae}
20	−10	0.8366	61.5561	0.5779	0.4058	58.0414	0.6594	0.4058	53.3249	0.7475
	0	0.3847	55.0000	0.4903	0.4058	50.3220	0.5721	0.4058	43.9653	0.6660
	10	0.0471	51.0568	0.4467	0.4058	45.6987	0.5312	0.4058	38.5188	0.6331
	20	0.4168	48.1495	0.4269	0.4058	42.3072	0.5168	0.4058	34.6329	0.6303
30	−15	0.3692	65.1039	0.4161	0.4043	62.1685	0.4893	0.4043	58.7234	0.5682
	0	0.1204	60.0000	0.3333	0.4043	56.1008	0.4023	0.4043	51.4480	0.4804
	15	0.0726	56.8598	0.3014	0.4043	52.3043	0.3718	0.4043	46.8548	0.4551
	30	0.9456	54.3429	0.2972	0.4043	49.2155	0.3748	0.4043	43.0926	0.4714
40	−20	0.2085	68.7680	0.2837	0.4029	66.0664	0.3464	0.4029	63.0939	0.4144
	0	0.7630	65.0000	0.2174	0.4029	61.4559	0.2734	0.4029	57.4747	0.3372
	20	0.5737	62.6013	0.1994	0.4029	58.4240	0.2571	0.4029	53.6694	0.3259
	40	0.7351	60.4258	0.2102	0.4029	55.5817	0.2789	0.4029	49.9888	0.3660

A. 3. Magnitudes of K_{ae}, t_c and α for $k_v=k_h$

		$k_h=0.0$			$k_h=0.1$			$k_h=0.2$		
Φ (°)	δ (°)	t_c (t)	α (°)	K_{ae}	t_c (t)	α (°)	K_{ae}	t_c (t)	α (°)	K_{ae}
20	−10	0.8366	61.5561	0.5779	0.3937	58.1426	0.6572	0.3937	53.6135	0.7427
	0	0.3847	55.0000	0.4903	0.3937	50.4574	0.5698	0.3937	44.3565	0.6608
	10	0.0471	51.0568	0.4467	0.3937	45.8531	0.5289	0.3937	38.9558	0.6273
	20	0.4168	48.1495	0.4269	0.3937	42.4746	0.5142	0.3937	35.0924	0.6236
30	−15	0.3692	65.1039	0.4161	0.3884	61.9800	0.4939	0.3884	58.2625	0.5781
	0	0.1204	60.0000	0.3333	0.3884	55.8484	0.4067	0.3884	50.8191	0.4905
	15	0.0726	56.8598	0.3014	0.3884	52.0088	0.3764	0.3884	46.1192	0.4662
	30	0.9456	54.3429	0.2972	0.3884	48.8827	0.3800	0.3884	42.2699	0.4846
40	−20	0.2085	68.7680	0.2837	0.3845	65.6817	0.3553	0.3845	62.2188	0.4339
	0	0.7630	65.0000	0.2174	0.3845	60.9455	0.2816	0.3845	56.2860	0.3561
	20	0.5737	62.6013	0.1994	0.3845	57.8179	0.2657	0.3845	52.2392	0.3470
	40	0.7351	60.4258	0.2102	0.3845	54.8729	0.2895	0.3845	48.2945	0.3940

Further information on retaining walls can be found in [15, 16, 17].

APPENDIX B

B. 1. Two dimensional ray tracing.

Consider Fig. App. B.1.

$$\boldsymbol{t} = -\boldsymbol{n}.\sqrt{1-\frac{n_d^2}{n_t^2}sin^2(\theta)} + \frac{n_d}{n_t}(\boldsymbol{d} - (\boldsymbol{d}.\boldsymbol{n}).\boldsymbol{n}) \tag{B-1}$$

Notice that $\boldsymbol{n}$ and $\boldsymbol{d}$ must be normalized vectors.

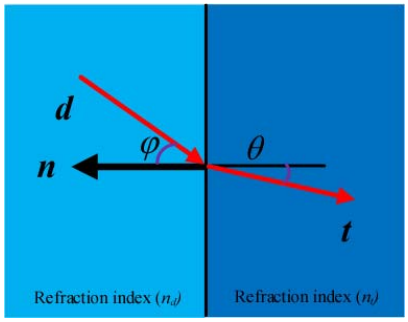

App. B.1. Ray tracing in 2D space

B. 2. Three dimensional ray tracing.

Define $\boldsymbol{i}^*$ and $\boldsymbol{j}^*$ as follows:

$$\boldsymbol{i}^* = \boldsymbol{n}$$

$$\boldsymbol{j}^* = \begin{cases} \dfrac{(\boldsymbol{n}+\dfrac{\boldsymbol{d}}{-\boldsymbol{n}.\boldsymbol{d}})}{norm(\boldsymbol{n}+\dfrac{\boldsymbol{d}}{-\boldsymbol{n}.\boldsymbol{d}})} & -1 \le \boldsymbol{n}.\boldsymbol{d} < -0.05 \\ \boldsymbol{d} & -0.05 \le \boldsymbol{n}.\boldsymbol{d} \le 0.05 \\ \dfrac{(\boldsymbol{n}-\dfrac{\boldsymbol{d}}{\boldsymbol{n}.\boldsymbol{d}})}{norm(\boldsymbol{n}-\dfrac{\boldsymbol{d}}{\boldsymbol{n}.\boldsymbol{d}})} & 0.05 < \boldsymbol{n}.\boldsymbol{d} \le 1 \end{cases} \tag{B-2}$$

Now define $\boldsymbol{n}^*$ and $\boldsymbol{d}^*$as:

$$\begin{aligned} \boldsymbol{n}^* &= (1,0) \\ \boldsymbol{d}^* &= (\boldsymbol{d}.\boldsymbol{i}^*, \boldsymbol{d}.\boldsymbol{j}^*) \end{aligned} \tag{B-3}$$

Calculate $\boldsymbol{t}^*$:

$$\boldsymbol{t}^* = -\boldsymbol{n}^* . \sqrt{1 - \frac{n_d^2}{n_t^2} sin^2(\theta)} + \frac{n_d}{n_t} (\boldsymbol{d}^* - (\boldsymbol{d}^* . \boldsymbol{n}^*) . \boldsymbol{n}^*) \tag{B-4}$$

Notice that $\boldsymbol{n}^*$ and $\boldsymbol{d}^*$ must be normalized vectors.

$\boldsymbol{t}^*$ is a two dimensional vector like $\boldsymbol{t}^*=(t_1^*, t_2^*)$.

Finally calculate $\boldsymbol{t}$:

$$\boldsymbol{t} = t_1^* . \boldsymbol{i}^* + t_2^* . \boldsymbol{j}^* \tag{B-5}$$

APPENDIX C

C. 1. Stability control

All the loads acting on the cantilever retaining wall are shown in Fig. App. C.1.

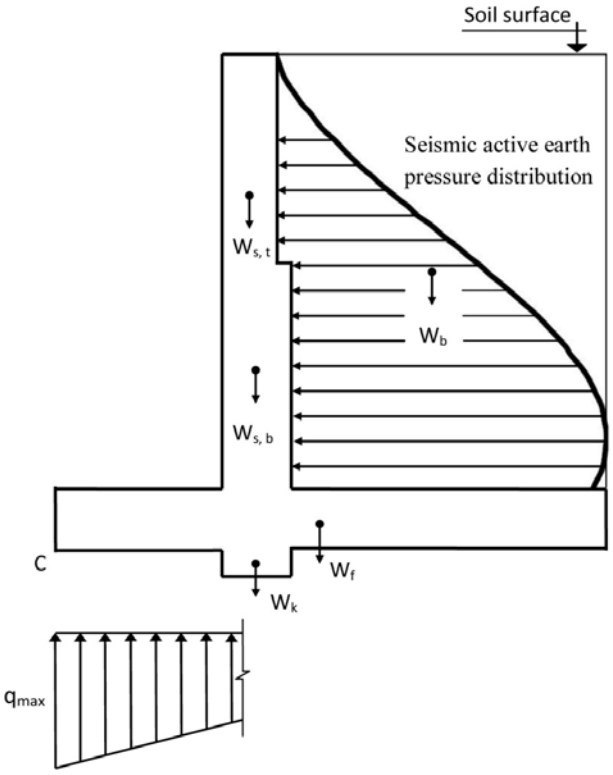

App. C.1. Loads on the cantilever retaining wall

Check for overturning:

$$FS_{overturning} = \frac{\sum M_r}{\sum M_o} \geq 1.5 \tag{C-1}$$

$\sum M_r$: Sum of the moments of forces that tends to resist the overturning of the wall about C.

$\sum M_o$: Sum of the moments of forces that tends to overturn the wall about point C.

Check for sliding along the base:

$$FS_{sliding} = \frac{P_{ae}}{\mu.\sum W} \geq 1.5 \tag{C-2}$$

P_{ae} : Total seismic active thrust.

$$\mu = tan(\varphi)$$

Check for bearing capacity failure:

$$FS_{\text{bearing capacity}} = \frac{q_u}{q_{max}} \geq 2 \tag{C-3}$$

q_u : Ultimate bearing capacity. It should be noticed that because of the existence of earthquake loading, the ultimate bearing capacity is increased by 33%.

q_{max} : Maximum bearing pressure.

$$q_{max} = \begin{cases} \dfrac{\sum W(1+\dfrac{6e}{L})}{BL}, for \quad e \leq \dfrac{L}{6} \\ \dfrac{2\sum W}{3B(0.5L-e)}, for \quad e > \dfrac{L}{6} \end{cases} \tag{C-4}$$

$$e = \frac{L}{2} - \frac{\sum Wx - M_{ae}}{\sum W}$$

where L is the footing length, B is the footing width which is equal to 1m , x is the length of the lever of the force about point C, and M_{ae} is the total moment of the seismic active thrust about point C.

C. 2. Strength control

The load combination is defined as the following, Ref. [13]:

$$\begin{aligned} M_u &= 1.2M_D + 1.4M_E \\ V_u &= 1.2V_D + 1.4M_E \end{aligned} \tag{C-5}$$

M_u and V_u are the ultimate moment and shear at the critical sections. The critical sections of the moment are shown in Fig. (3). The critical sections of the shear are at a distance d (effective depth) from the face of moment critical sections.

Check the shear capacity:

$$\frac{V_u}{\Phi_v.V_n} \leq 1 \tag{C-6}$$

$$V_n = \frac{\sqrt{f_c}}{6}.B.d \tag{C-7}$$

B is the length of shear critical section based on (mm), which is equal to 1000mm, ϕ_v is equals 0.75, d is the effective depth, (mm) and f_c is the concrete strength (MPa).

Determining the required rebar:

Based on M_u (N.mm) in each critical cross section, the required area cross section of rebar, A_s based on (mm), is calculated. The minimum steel ratio is 0.0018.

$$m = \frac{f_y}{0.85 f_c}$$
$$R_n = \frac{M_u}{\Phi_b . B . d^2} \tag{C-8}$$
$$A_s = \frac{B.d}{m}\left\{1 - \sqrt{1 - \frac{2m.R_n}{f_y}}\right\}$$

ϕ_b is equal to 0.9 and f_y is the rebar yield stress in MPa.